

Chapter 3

**Effect of Spacer Chain Length on Aggregation
Properties of Alkanediyl- α,ω -bis (dodecyl
hydroxyethyl methyl ammonium bromide) Bis-
cationic Surfactants**

Contents

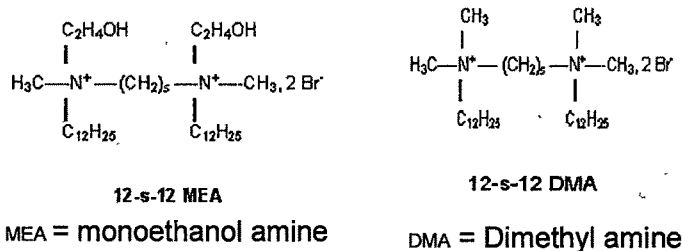
	Page no.
3.1 Introduction	121
3.2 Experimental	122
3.2.1 Materials	123
3.2.2 Synthesis and characterization of surfactants	123
3.2.3 Procedure	125
3.3 Results and Discussion	125
3.3.1 Kraft temperature	125
3.3.2 Critical micelle concentration	126
3.3.3 Thermodynamic parameters of micellization	130
3.3.4 SANS and micellar solutions	134
Effect of spacer chain length	
Effect of temperature	
3.3.5 Viscosity of micellar solutions	140
3.3.6 Foamability and foam stability	142
3.4 Conclusions	143
3.5 Literature Cited	144 - 145

3.1 Introduction

A new generation gemini surfactants show very low critical micellar concentration (CMC), better wetting properties, lower limiting surface tension and unusual aggregation morphologies [1-11], as compared to conventional monomeric surfactants. Surfactant molecules above critical micellar concentration (CMC) in aqueous solution are known to form variety of microstructures such as spherical, ellipsoidal, vesicular, rod-like and thread-like [12-19]. The microstructure of surfactant aggregates depends on molecular architecture of surfactant and conditions such as concentration and temperature [12-17]. The bis-cationic surfactants where two long chains of ter-amines are covalently attached through the polymethylene spacer at the head group have been recently well studied [19 -24]. The physicochemical properties of bis-cationic surfactant molecules primarily depend upon the structure of molecules under consideration as seen in more than 10 times decrease in CMC, when two DTAB molecules are covalently connected through polymethylene spacer at the head group level [7,20]. Moreover, the microstructure of micelles and physicochemical properties of bis-cationic surfactants depend on nature and length of spacer which has been examined for different types of spacers such as polymethylene, polyoxyethylene, and aromatic rings [21-25]. Zana and coworkers [19, 20] studied micellar solutions of conventional bis-cationic surfactants 12-s-12 DMA through Cryo-Transmission electron microscopy. They have reported that surfactant with spacer chain length 2 and 3 show long thread-like micelles, while nearly spherical micelles are formed with spacer chain length 4 and 6. SANS studies of alkanediyl- α, ω -bis(alkyldimethyleammonium bromide) type of bis-cationic surfactants containing $-N(CH_3)_2$ head groups and C_{10} , C_{16} alkyl chain lengths have been extensively reported[22,25]. Wang et al [21] have reported that the microstructure of surfactant aggregates and thermodynamic properties of micellization of gemini surfactants with fixed alkyl chain and spacer length strongly depend on the nature and conformation of spacer at micelle-water interface and observed that gemin surfactants with a hydrophilic flexible spacer form more closely packed micellar structure than the one with

hydrophobic rigid spacer. Wettig et al [9,10, 22] have also reported that the aggregation behavior of gemini surfactant strongly depends on nature and length of spacer chain.

Hence in this chapter we report the synthesis, characterization and effect of variation in spacer chain length on aggregation behavior of alkanediyl- α,ω -bis (dodecyl hydroxyethyl methyl ammonium bromide) surfactant. The general structure of these surfactant is



where s = 4, 6, 8 and 10

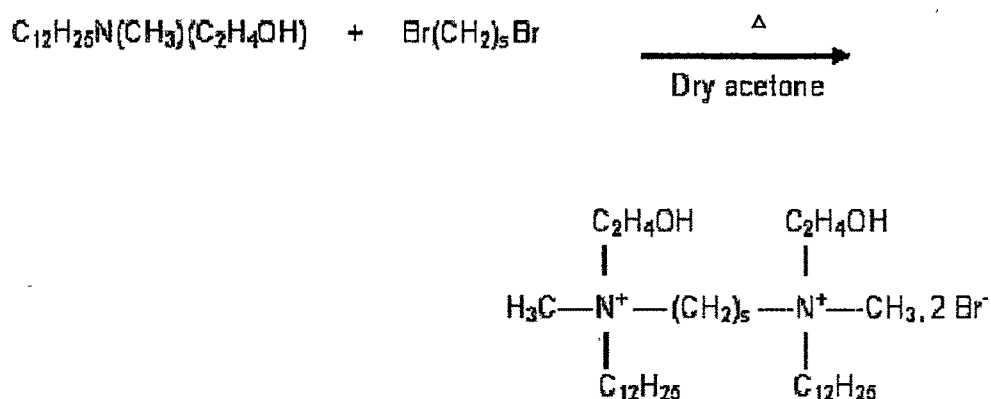
3.2 Experimental

3.2.1 Materials

n-Dodecyl bromide, α,ω -dibromoalkane and 2(methylamino)ethanol were purchased from Lancaster Chemical Company, Morecambe, England. All the reagents and solvents used were of AR grade. Solutions for SANS studies were prepared in D₂O (at least 99 atom % D) obtained from Heavy Water Division, Bhabha Atomic Research Centre, Mumbai, India. Double-distilled and deionized water was used for all physicochemical studies.

3.2.2 Synthesis of Dimeric Surfactants and Characterization

The 12-s-12 MEA surfactants were synthesized by refluxing 2.2 moles of dodecyl hydroxyethylmethyl amine in dry acetone with 1.0 mole of α,ω -dibromo alkane for 70 h., at 58 - 60°C.



(where $s = 4, 6, 8$ and 10)

The solvent from reaction mixture was removed under vacuum and the crude white solid thus obtained was purified by washing with hexane/ethyl acetate mixture and recrystallized from acetone/methanol mixture for at least three times to obtain pure compound. The overall yield of the surfactant was observed to be 70 - 80 %. The identity and purity of the final product was confirmed by TLC, elemental, FTIR and ^1H NMR analysis.

FTIR spectra of the surfactants were recorded in KBr pellets using Perkin Elmer FTIR Spectrophotometer RX, of resolution 2 cm^{-1} . The absorption bands were observed at $3401\text{-}3656 \text{ cm}^{-1}$ (OH stretching), 2916 cm^{-1} (CH stretching), 1108 cm^{-1} (CN stretching), 1084 cm^{-1} (CO stretching) and 720 cm^{-1} (CH stretching of long alkyl chain).

Elemental analysis and ^1H NMR spectra of products in CDCl_3 were recorded using Perkin Elmer Series II elemental analyzer and 300 MHz Bruker NMR Spectrophotometer respectively.

Butanediyl-1,4,-N,N'-bis(dodecyl hydroxyethyl methyl ammonium bromide) represented as **12-4-12 MEA**, ^1H NMR spectrum in CDCl_3 , showed signal at δ 0.84 ppm (t, 6H 2CH_3 alkyl chain), 1.25-1.40 ppm (br m, 36H, 18CH_2 alkyl chain), 1.75 ppm (m, 4H, 2CH_2 alkyl chain), 2.1 ppm (m, 4H, 2CH_2 spacer

chain), 3.25 ppm (s, 6H, $2\text{N}^+\text{CH}_3$), 3.62 ppm (t, 12H, $2\text{xN}^+(\text{CH}_2)_3$), 3.82 ppm (t, 4H, $2\text{CH}_2\text{-OH}$) and 4.18 ppm (s, 2H, 2OH).

Percentage of C, H, N calculated for $\text{C}_{34}\text{H}_{74}\text{N}_2\text{O}_2\text{Br}_2$ was C: 58.10, H: 10.61, N: 3.98 and experimentally observed was C: 58.20, H: 10.75, N: 4.01 %.

Melting point of the surfactant was observed to be $195 \pm 2^\circ\text{C}$.

Hexanediyl-1,6-N-N'-bis(dodecyl hydroxyethyl methyl ammonium bromide)

represented as **12-6-12 MEA**, ^1H NMR spectrum in CDCl_3 , exhibited signal at δ 0.84 ppm (t, 6H, 2CH_3 alkyl chain), 1.25 ppm (br m, 40H, 20CH_2 alkyl chain), 1.65 ppm (m, 4H, 2CH_2 spacer chain), 1.95 ppm (m, 4H, 2CH_2 spacer chain), 3.25 ppm (s, 6H, $2\text{N}^+\text{CH}_3$), 3.59 ppm (t, 12H, $2\text{N}^+(\text{CH}_2)_3$), 3.75 ppm (t, 4H, $2\text{CH}_2\text{-OH}$), 4.15 ppm (s, 2H, 2OH).

Percentage of C, H, N calculated for $\text{C}_{36}\text{H}_{78}\text{N}_2\text{O}_2\text{Br}_2$ was C: 59.16, H: 10.75, N: 3.83 and experimentally observed was C: 59.49, H: 10.86, N: 4.00 %

Melting point of the surfactant was observed to be $206 \pm 2^\circ\text{C}$.

Octanediyl-1,8-N-N'-bis(dodecyl hydroxyethyl methyl ammonium bromide)

represented as **12-8-12 MEA**, ^1H NMR spectrum in CDCl_3 , showed signal at δ 0.81 ppm (t, 6H, 2CH_3 alkyl chain), 1.17 ppm (br m, 40H, 20CH_2 alkyl chain), 1.35 ppm (t, 8H, 4CH_2 spacer chain), 1.74 ppm (m, 4H, 2CH_2 spacer chain), 3.20 ppm (s, 6H, $2\text{N}^+\text{CH}_3$), 3.59 ppm (t, 12H, $2\text{N}^+(\text{CH}_2)_3$), 3.93 ppm (t, 4H, $2\text{CH}_2\text{-OH}$), 3.99 ppm (s, 2H, 2OH).

Percentage of C, H, N calculated for $\text{C}_{38}\text{H}_{82}\text{N}_2\text{O}_2\text{Br}_2$ was C: 60.14, H: 10.89, N: 3.69 and experimentally observed was C: 60.32, H: 11.00, N: 3.73 %.

Melting point of the surfactant was observed to be $193 \pm 2^\circ\text{C}$.

Decanediyl-1,10-N-N'-bis(dodecyl hydroxyethyl methyl ammonium bromide)

represented as **12-10-12 MEA**, ^1H NMR spectrum in CDCl_3 , exhibited signal at δ 0.81 ppm (t, 6H, 2CH_3 alkyl chain), 1.30 ppm (m, 40H, 20CH_2 alkyl chain), 1.35 ppm (t, 8H, 4CH_2 spacer chain), 1.70 ppm (m, 8H, 4CH_2 spacer chain), 3.20 ppm (s, 6H, $2\text{N}^+\text{CH}_3$), 3.59 ppm (t, 12H, $2\text{N}^+(\text{CH}_2)_3$), 3.93 ppm (t, 4H, $2\text{CH}_2\text{-OH}$), 3.99 ppm (s, 2H, 2OH).

chain), 3.24 ppm (s, 6H, $2\text{N}^+\text{CH}_3$), 3.67 ppm (t, 12H, $2 \times \text{N}^+(\text{CH}_2)_3$), 4.05 ppm (t, 4H, $2\text{CH}_2\text{-OH}$), 5.12 ppm (s, 2H, 2OH).

Percentage of C, H, N calculated for $\text{C}_{40}\text{H}_{86}\text{N}_2\text{O}_2\text{Br}_2$ was C: 61.05, H: 11.02, N: 3.56 and experimentally observed was C: 61.25, H: 11.10, N: 3.60 %.

Melting point of the surfactant was observed to be $203 \pm 2^\circ\text{C}$.

3.2.3 Procedure

The measurements of conductance, surface tension, intrinsic viscosity, density, foamability, foam stability and SANS were done following the procedures described in section 2.2. Absolute viscosities of aqueous solutions of surfactants were determined as a function of shear rate, temperature, surfactant concentration and spacer chain length, using Brook Field DV-III digital cone and plate rheometer. The diameter of the cone was 40 mm and the cone angle was 0.8° . To ensure the reproducibility of the measurements, great care was exercised when sample was introduced into the rheometer to avoid shear effect on the solution. Measurements were repeated two times on fresh solutions and were found to be reproducible within 2%. The measuring device was equipped with a Peltier Plate temperature unit for good temperature control over an extended time.

3.3 Results and Discussion

3.3.1 Kraft Temperature

The Kraft temperatures (k_T) of 12-s-12 MEA gemini surfactants were measured as a function of spacer chain length through conductance measurement as described earlier in section 2.2.2 and are given in Table 3.1. All surfactants showed k_T below zero except the surfactant with spacer length 4 i.e. 12-4-12 MEA. Similar trend is reported for homologues series of cationic gemini surfactant (12-s-12 DMA) [26, 27]. In general dimeric surfactants show higher k_T than the corresponding monomeric ones, as observed in 16-2-16 DMA and CTAB (45 and 25°C respectively) and 12-2-12 DMA and DTAB (15 and 0°C respectively)[26]. However, dimeric surfactants derived from

arginine showed lower k_T values lower than their corresponding monomeric counterpart [28].

Table 3.1 Kraft temperatures of 12-s-12 MEA series of surfactants

Surfactants	Kraft temp., k_T ($^{\circ}\text{C}$)
12-4-12 MEA	30
12-6-12 MEA	< 0
12-8-12 MEA	< 0
12-10-12 MEA	< 0

3.3.2 Critical Micelle Concentration (CMC)

The CMC values for 12-s-12 MEA series of bis-cationic surfactants were determined by surface tension and conductivity measurements. The CMC values obtained from both the techniques show same trend with spacer chain length and are given in Table 3.2. It is interesting to note that CMC data of the 12-s-12 MEA bis-cationic surfactants are observed to be 10-100 times lower than the conventional 12-s-12 DMA bis-cationic surfactants. For 12-s-12 MEA, the oxygen atom of $-\text{C}_2\text{H}_4\text{OH}$ groups can form hydrogen bond with water, providing hydration at the head group level, which screens-out the Coulombic repulsion between the charged heads. This helps 12-s-12 MEA surfactant to form aggregates at a lower concentration than that of 12-s-12 DMA surfactant.

Figure 3.1, shows that CMC goes on increasing with the spacer chain length up to 6 carbon atoms and thereafter decreases with increase in the spacer length. Similar trend has also been reported by Zana and coworker [8,11]. The variation in CMC with spacer chain length can be attributed to the conformational changes taking place with polymethylene spacer. For spacer chain, $s = 6$, spacer remains fully in extended conformation and makes slightly more difficult for the spacer to locate at micelle-water interface, while for longer spacers $s > 6$, they try to fold inside the hydrophobic core establishing

a probable attractive hydrophobic interaction between the tails and spacer. The average degree of ionization of counterions of the micelles was observed to be less than those of conventional bis-cationic surfactants (12-s-12 DMA) and increase with increase in spacer length (Table 3.2).

The surface active parameters such as surface excess concentration of surfactant (Γ_{\max}) and minimum area per molecule at air-water interface (A_{\min}), determined from surface tension data using equations 4 and 5 from section 2.3.5 and are given in Table 3.2. From the Table 3.2, it is observed that the CMC and A_{\min} values were observed to be maximum and Γ_{\max} value minimum for a spacer chain length of 6 methylene units. The variation of micellar parameters with spacer length can be attributed to conformational changes of spacer at micelle-water interface. Zana [24] and De et al [29] also observed similar trend in dependence of micellar parameters on spacer chain length for 12-s-12 DMA and 16-s-16 DMA gemini surfactants respectively.

The Gibb's free energy changes of micellization (ΔG°_m) and Gibb's free energy changes of adsorption (ΔG°_{ad}) were calculated by using equation 1 and 6 from section 2.3.4 and 2.2.5 and are given in Table 3.2. The difference between ΔG°_{ad} and ΔG°_m is considered as effective Gibb's free energy change of micellization and is represented as ΔG°_{eff} . It is also called as energy barrier between the two different processes micellization and adsorption. The ΔG°_{eff} value was observed to be smaller for spacer chain length 4 than that for spacers 6, 8 and 10. This indicates that the surfactant with shorter spacer shows higher aggregation tendency than that with longer spacer (6, 8 and 10).

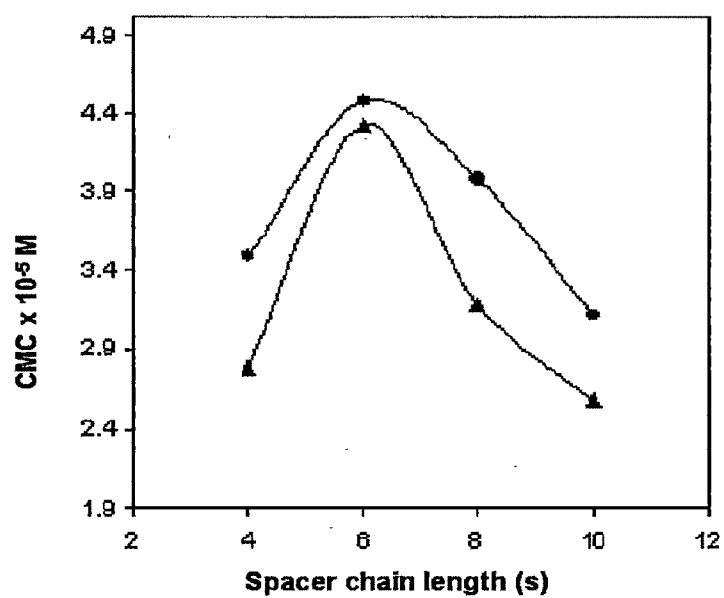


Figure 3.1 Effect of spacer chain length on critical micelle concentration of 12-s-12 MEA series of bis-cationic surfactants at 30°C. by conductometry (●), by tensiometry (▲)

Table 3.2 Critical micellar concentration (CMC), average degree of ionization (α_{ave}), surface excess concentration (Γ_{max}), minimum area per molecule at air/water interface (A_{min}) and Gibb's free energy of change of micellization (ΔG_m°), Gibb's free energy change of adsorption (ΔG_{ad}°), effective Gibb's free energy change of micellization (ΔG_{eff}°) of 12-s-12 MEA bis-cationic surfactants, at 30°C.

Spacer length (s)	CMC by tensiometry ($\times 10^{-5}$ M)	(α_{ave})	($-\Delta G_m^\circ$) KJ.Mole ⁻¹	CMC by conductometry ($\times 10^{-5}$ M)	A_{min} (Å ²)	Γ_{max} ($\times 10^{-10}$)	($-\Delta G_{ad}^\circ$) KJ.Mole ⁻¹	($-\Delta G_{eff}^\circ$) KJ.Mole ⁻¹
4	3.49±0.10	0.26 (0.31)	32.78	2.78 ± 0.10 (117 ± 10)	155	1.08	43.25	10.47
6	4.49±0.10	0.31 (0.33)	30.12	4.33 ± 0.10 (103 ± 10)	193	0.86	41.54	11.42
8	3.99±0.15	0.36 (0.45)	29.74	3.18 ± 0.10 (83 ± 10)	162	1.03	41.96	12.22
10	3.12±0.10	0.39 (0.54)	29.53	2.59 ± 0.10 (63 ± 10)	154	1.08	42.02	12.49

(Note: The values given in bracket are of conventional bis-cationic surfactant $C_{12}H_{25}N^+(CH_3)_2-(CH_2)_s-(CH_3)_2N^+C_{12}H_{25}$, taken from reference 8.)

3.3.3 Thermodynamic Parameters of Micellization

The thermodynamic parameters of micellization such as ΔG_m° , ΔH_m° and ΔS_m° at different temperatures for surfactants with variable spacer length are determined by using equations 1, 2 and 3 from section 2.3.4 and are given in Table 3.3. The observed more negative ΔG_m° value for the surfactant with shorter spacer of 4 units indicates more favored micellization. Negative values of enthalpy (ΔH_m°) of micellization indicate exothermic nature of micellization process. Nusselder and Engbert's [30] have suggested that for the negative ΔH_m° the dispersion forces play major role in the micelle formation. Also, the observed exothermicity can be attributed to possible surfactant-solvent interactions. The enthalpy values do not vary significantly with temperature, indicating no significant variation in the environment surrounding the hydrocarbon chain of the surfactant molecule with temperature. The entropy of micellization (ΔS_m°) being more positive, in the system under study, micellization is entropy (ΔS_m°) driven. The more positive values of entropy may be due to the breaking of bulk water structure around the molecules. This leads to more disorder in the structure of water and favors the micellization at lower concentration. More positive entropy values indicate micellization process to be more spontaneous. High entropy changes are generally associated with a phase change. Hence it can be assumed that the micelles form separate phase in these systems. The observed sharp increase in the entropy values, indicates that shorter spacer ($s = 4$) favors micellization process more than larger spacer ($s = 6, 8$ and 10).

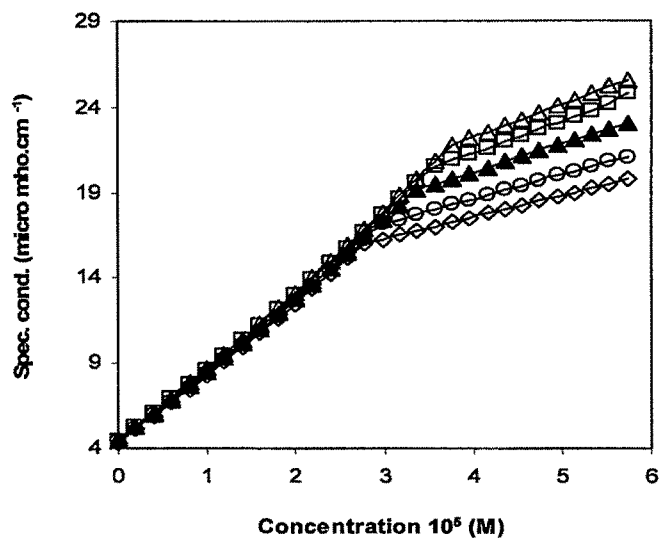


Figure 3.2(a) Effect of temperature on 12-4-12 MEA bis cationic surfactant, 30 (\diamond), 35 (\circ), 40 (\blacktriangle), 45 (\square) and 50 $^{\circ}\text{C}$ (\triangle)

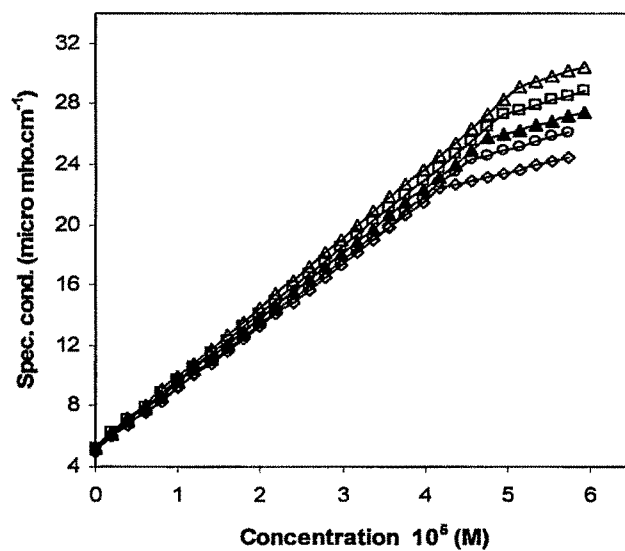


Figure 3.2(b) Effect of temperature on 12-6-12 MEA bis cationic surfactant, 30 (\diamond), 35 (\circ), 40 (\blacktriangle), 45 (\square) and 50 $^{\circ}\text{C}$ (\triangle)

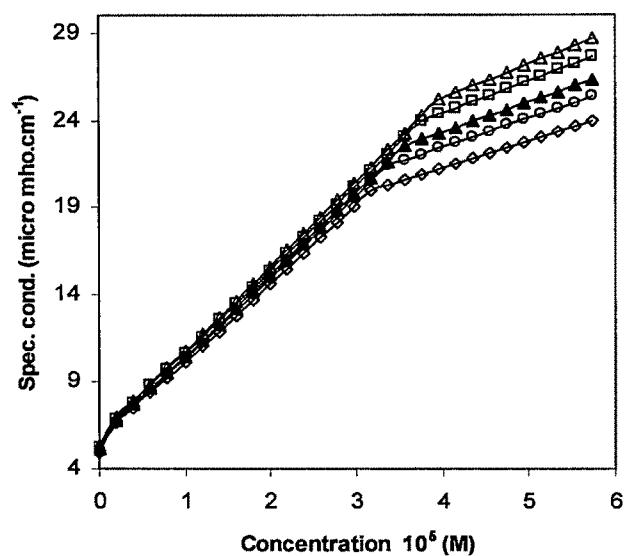


Figure 3.2(c) Effect of temperature on 12-8-12 MEA bis cationic surfactant,
30 (\diamond), 35 (\circ), 40 (\blacktriangle), 45 (\square) and 50 $^{\circ}\text{C}$ (\blacktriangledown)

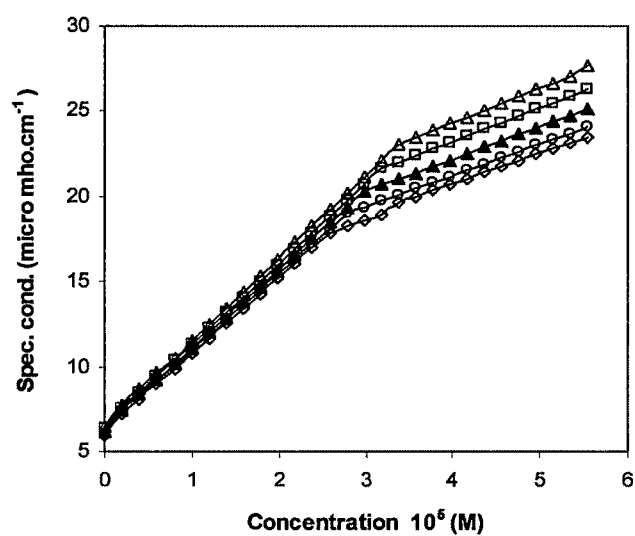


Figure 3.2 (d) Effect of temperature on 12-10-12 MEA bis-cationic surfactant,
30 (\diamond), 35 (\circ), 40 (\blacktriangle), 45 (\square) and 50 $^{\circ}\text{C}$ (\blacktriangledown)

Table 3.3 Effect of spacer chain length and temperature on thermodynamic parameters of micellization of bis-cationic surfactants

Surfactant system	Temperature (°C.)	Gibb's Free energy (- ΔG_m^0) KJmol ⁻¹	Enthalpy (- ΔH_m^0) KJmol ⁻¹	Entropy (ΔS_m^0) Jk ⁻¹ mol ⁻¹
12-4-12 MEA	30	32.77 \pm 1.5	14.96 \pm 0.9	58.78 \pm 1.2
	35	32.01 \pm 1.5	14.95 \pm 0.9	55.39 \pm 1.2
	40	31.05 \pm 1.5	14.93 \pm 0.9	51.50 \pm 1.2
	45	30.59 \pm 1.5	15.01 \pm 0.9	48.99 \pm 1.2
	50	30.36 \pm 1.5	15.21 \pm 0.9	46.88 \pm 1.2
12-6-12 MEA	30	30.00 \pm 1.5	13.28 \pm 0.9	55.18 \pm 1.2
	35	29.95 \pm 1.5	13.61 \pm 0.9	53.03 \pm 1.2
	40	29.95 \pm 1.5	13.93 \pm 0.9	51.18 \pm 1.2
	45	29.95 \pm 1.5	14.24 \pm 0.9	49.40 \pm 1.2
	50	29.95 \pm 1.5	14.58 \pm 0.9	47.58 \pm 1.2
12-8-12 MEA	30	29.38 \pm 1.6	15.66 \pm 0.9	45.28 \pm 1.3
	35	29.28 \pm 1.6	16.04 \pm 0.9	42.98 \pm 1.3
	40	29.23 \pm 1.6	16.42 \pm 0.9	40.92 \pm 1.2
	45	29.18 \pm 1.6	16.79 \pm 0.9	38.96 \pm 1.2
	50	29.18 \pm 1.7	16.17 \pm 0.9	37.18 \pm 1.2
12-10-12 MEA	30	29.19 \pm 1.6	18.63 \pm 0.9	34.85 \pm 1.3
	35	29.12 \pm 1.6	19.08 \pm 0.9	32.59 \pm 1.3
	40	29.02 \pm 1.6	19.53 \pm 0.9	30.32 \pm 1.2
	45	28.89 \pm 1.6	19.97 \pm 0.9	28.05 \pm 1.2
	50	28.82 \pm 1.7	20.41 \pm 0.9	26.04 \pm 1.2

3.3.4 SANS and Micellar Solutions

Effect of Spacer Chain Length

To understand the effect of head polarity and spacer chain on microstructure of surfactant aggregates in aqueous solution, SANS measurements were carried out at 100 mM solution of 12-s-12 MEA surfactant with spacers (s) = 4, 6, 8 and 10. SANS distributions (Fig. 3.3) show well defined correlation peaks irrespective of the spacer chain length, due to the inter-micellar structure factor $S(Q)$. The correlation peaks appear at around $Q_{\max} \simeq 2\pi/D$, where D is average distance between micelles. Increase in Q_{\max} with spacer length at the same surfactant concentration indicates the increased number density (n) of micelles. It is observed from Figure 3.3 that the peak positions shift towards higher Q values with increase in spacer chain length from 4 to 6. However, the shift in Q is small with the further change in spacer chain length from 6 to 10. The observed SANS data were analyzed for aggregation number (N), fractional charge (α), semi-minor axis (a) taking fitting parameters and the semi-major axis (b) was calculated by using knowledge of above parameters $b = 3Nv/4\pi a^2$. The extracted micellar parameters values are given in Table 3.4.

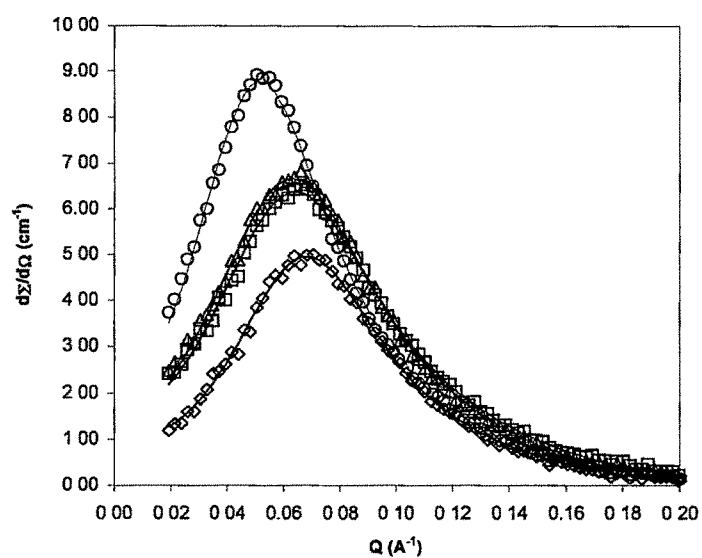


Figure 3.3 Effect of spacer chain length on SANS distribution for 12-s-12 MEA bis-cationic surfactant at 100 mM concentrations and 30°C. $s = 4$ (o), 6 (Δ), 8 (\square), 10 (\diamond).

Table 3.4 Effect of spacer chain length (s) on micellar parameters of 12-s-12 MEA bis-cationic surfactants of 100 mM at 30 °C.

Spacer length s	Aggregation number N	Fractional charge α	Semi-minor axis, a (Å)	Semi-major axis, b (Å)	Equilibrium distance between heads d(Å)	b/a	Hydration of micelle $h_m(\text{cm}^3/\text{g})$
4	108 \pm 8	0.11 \pm 0.01	18.6 \pm 0.5	78.6 \pm 1.8	7.26 (7.56)	4.2	0.912
6	56 \pm 5	0.18 \pm 0.01	16.4 \pm 0.5	55.3 \pm 1.4	8.23 (10.64)	3.3	0.398
8	55 \pm 5	0.19 \pm 0.01	17.3 \pm 0.5	51.3 \pm 1.3	8.46 (13.74)	3.0	0.258
10	52 \pm 4	0.24 \pm 0.01	17.6 \pm 0.5	48.7 \pm 1.3	8.68 (16.80)	2.8	0.246

(Note: The values given in parentheses are the theoretically calculated distances between the charged heads of the gemini surfactant molecules.)

The equilibrium distance between the charged heads (d) was calculated for bis-cationic surfactants under study with respect to spacer length and are given in Table 3.4. Significant decrease in aggregation number (N) and increase in fractional charge (α) was observed when spacer chain length increased from 4 to 6 than when it increased from 6 to 8 and 10 (Table 3.4). This can be attributed to conformational changes in spacer at micelle-water interface. The spacer $s = 6$ remains in fully extended conformation whereas the spacer with > 6 units forms a loop extended towards hydrophobic core of micelle and subsequently disrupts the geometry's of micelle. The equilibrium distance between the charged head increases with increase in spacer chain length, resulting in the increase in the spontaneous packing curvature restricting the growth of micelle. Surfactant with shorter spacer of 4 carbon units forms bigger micelles in aqueous solution than surfactant with longer spacer (s) = 6, 8 & 10 (Table 3.4). This is also supported by observed shear thickening behavior of surfactant with spacer length of 4 carbons as shown in Figure 3.5. Zana et al [8,11] reported that the 12-s-12 DMA bis-cationic surfactant with spacer length 4 and 6 formed spherical micelle, while surfactants in the present study with more polar heads 12-s-12 MEA and spacer length 4 and 6 formed more elongated ellipsoidal micelles, indicating that the increase in head group polarity of surfactant increases aggregation tendency. The change in head group polarity and spacer length of bis-cationic surfactant results in a significant change in micellar geometry. We have observed b/a ratio to decrease from 4.2 to 2.8 with increase in spacer length from 4 to 10 indicating that the spacer length 4 shows higher tendency of aggregation than larger spacers 6, 8 and 10.

Effect of Temperature

Figure 3.4 shows SANS distribution for 100 mM of 12-4-12 MEA bis-cationic surfactant at 30, 45, and 60°C. Peak position in SANS was observed to be shifted to the higher Q values with overall decrease in the peak intensity and increase in broadness of peak, with increasing temperature. Similarly the correlation peak Q_{\max} was found to change with temperature, indicating the number density of micelle changes with temperature.

The micellar parameters in these systems are given in the Table 3.5. Increase in temperature of surfactant system increases fractional charge (α) and hence electrostatics repulsion between the surfactant heads. This results in decrease in aggregation number (N) and reduces dimension of micelle (b/a). Since smaller effective charge indicates a more ellipsoidal morphology, increasing temperature appears to induce some what ellipsoidal to sphere transition for 12-4-12 MEA micelles. This notation is also supported by the concomitant decrease in $b/a \sim 4.2$ to ~ 2.9 upon increase in temperature.

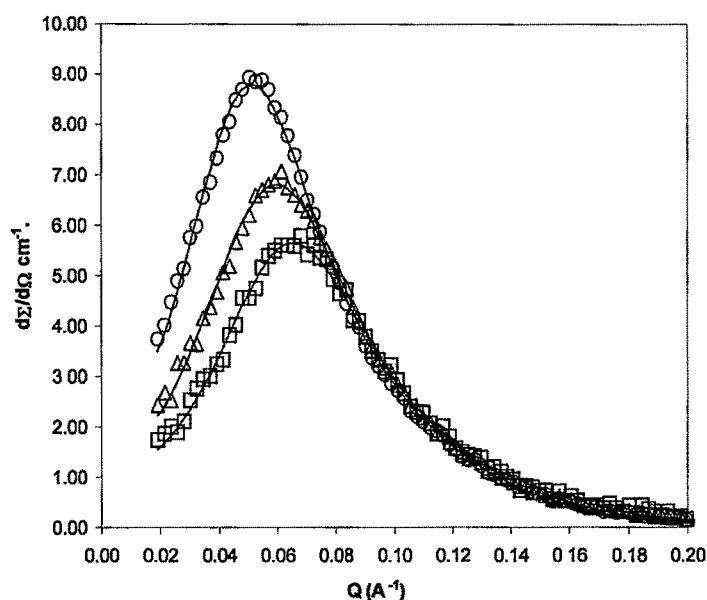


Figure 3.4 Effect of temperature on SANS distribution for 100 mM 12-4-12 MEA bis-cationic surfactant at various temperatures. 30°C (o), 45°C (Δ) and 60°C (\square).

Table 3.5 Effect of temperature on micellar parameters of 12-4-12 MEA bis-cationic surfactant at 100 mM concentration.

Temperature (°C)	Aggregation number N	Fractional charge α	Semi-minor axis, a (Å)	Semi-major axis, b (Å)	Axial ratio b/a
30	108 \pm 8	0.11 \pm 0.01	18.6 \pm 0.5	78.6 \pm 1.8	4.2
45	71 \pm 4	0.15 \pm 0.01	18.2 \pm 0.5	53.9 \pm 1.4	3.0
60	57 \pm 5	0.22 \pm 0.01	17.1 \pm 0.5	49.0 \pm 1.4	2.9

3.3.5 Viscosity of Micellar Solutions

Table 3.6 shows the viscosity data for 100 mM, 12-s-12 MEA bis-cationic surfactant with different spacer lengths. Surfactant with spacer length 4 showed very high absolute viscosity in comparison with the surfactant with spacer lengths 6, 8 and 10, indicating the formation of larger aggregates in aqueous solution. Figure 3.5, shows that the surfactant with shorter spacer chain $s = 4$, shows some what shear thickening behavior, whereas surfactants with spacer lengths 6, 8 and 10 carbon atoms show essentially Newtonian behavior. It is proposed that the shear thickening is a shear-induced phenomenon [31-33], and can be attributed to the interparticle hydrodynamic interaction. In the case of surfactant solutions under study existence of charged elongated ellipsoidal micelles results into increase in viscosity. Table 3.6, gives the viscosities at different concentrations and temperatures for surfactant with spacer length of 4 carbon atoms. As expected the viscosity decreases with decrease in the surfactant concentration or increase in the temperature.

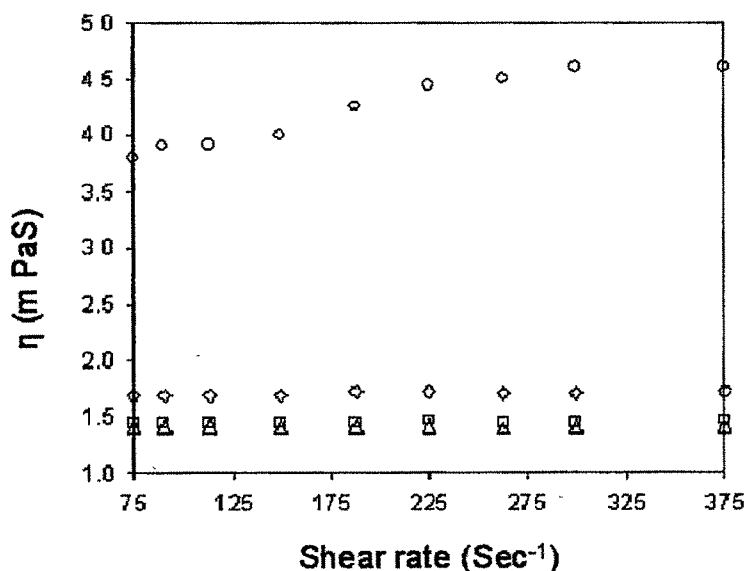


Figure 3.5 Effect of variation of shear rate on absolute viscosity of 12-s-12 MEA bis-cationic surfactant, at 100 mM concentration and 30°C. $s = 4$ (○), 6 (Δ), 8 (□), 10 (◇).

Table 3.6 Effect of spacer length, concentration and temperature on absolute viscosity's of 12-s-12 MEA bis-cationic surfactants in aqueous solutions.

Parameter	η in m PaS
(a) Effect of spacer chain length(s) on absolute viscosity of 12-s-12 MEA surfactants at 100mM and 30 °C.	
S = 4	4.60±0.09
6	1.42± 0.03
8	1.47± 0.03
10	1.72± 0.03
(b) Effect of concentrations on absolute viscosity for 12-4-12 MEA surfactant, at 30 °C temperature.	
100 mM	4.60± 0.09
75 mM	1.70± 0.03
50 mM	1.22± 0.02
25 mM	1.07± 0.02
(c) Effect of temperature on absolute viscosity, for 12-4-12 MEA surfactant at 100mM concentration.	
30°C	4.60± 0.09
35 °C	2.44± 0.05
40 °C	1.92± 0.04
45 °C	1.60± 0.03

3.3.6 Foamability and Foam Stability

Foamability and foam stability of 12-s-12 MEA gemini surfactant (1% w/v solution) was studied as per the method reported by Shah [34]. In this method foam is produced quickly by rapid shaking of cylinder containing surfactant solution causing a sudden expansion of interfacial area. The foamability and foam stability as a function of spacer is given in Fig. 3.6. Shorter spacer $s = 4$ shows less foamability and more foam stability than larger spacer $s = 6, 8$ and 10 . Foamability and foam stability can be influenced by two independent factors: molecular packing in adsorbed surfactant film at the air/water interface [35] and micelle structure within the bulk water in foam lamellae [36].

This can be explained on the basis of competitive time scales for interfacial area expansion, the diffusion transport of surfactant monomers and the ability of micelle to break up in order to provide monomer flux necessary to stabilize the new air/water interface. Surfactant with spacer $s = 4$ form bigger and compact micelle (Table 3.4) than that of larger spacer ($s = 6, 8$ & 10). This indicates, surfactant with spacer $s = 4$ has low monomer flux than that of larger spacer and hence 12-4-12 MEA shows low foamability and high foam stability.

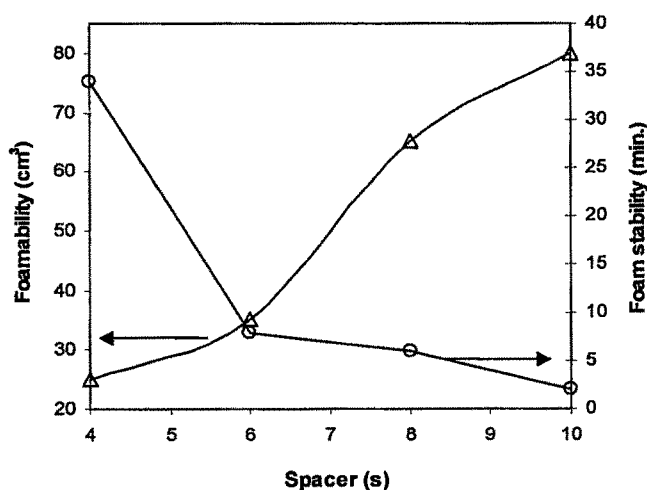


Figure 3.6 Foamability and foam stability of 12-s-12 MEA surfactant (1% w/v solution) as function of spacer(s) chain length at 30°C.

3.4 Conclusions

- A series of novel bis-cationic surfactants 12-s-12 MEA where two highly polar quaternary amine centers are connected through varying lengths of polymethylene spacers of 4, 6, 8 and 10 units at the head groups, has been synthesized and characterized.
- The presence of ethanolic groups at quaternary nitrogen increases the head polarity of the surfactants, resulting into reduction in the CMC, average degree of ionization (α_{ave}) and higher tendency of surfactant to aggregate, as compared to conventional 12-s-12 DMA bis-cationic surfactants.
- CMC of the surfactant increases up to spacer length 6 and then it decreases with further increase in spacer length.
- SANS data indicate that the surfactant with shorter spacer $s = 4$ shows higher aggregation tendency than that of larger spacer.
- Viscosity of 12-s-12 MEA surfactant with $s = 4$ shows higher viscosity than larger spacer $s = 6, 8$ and 10 .
- The flow curves of all 12-s-12 MEA surfactant show Newtonian behavior.
- It has also been found that the size of micelles decreases when the temperature is increased.

3.5 Literature Cited

1. Menger F. M., Littau C. A., *J. Am. Chem. Soc.*, **1991**, 113, 1451.
2. Menger F. M., Littau C. A., *J. Am. Chem. Soc.*, **1993**, 115, 10083.
3. Bunton C.A., Robinson L., Schaak J., Stern M. F., *J. Org. Chem.*, **1971**, 36, 2346.
4. Rosen M. J., *Chemtech*, **1993**, 23, 30.
5. Menger F. M., Keiper J. S., *Angewchem, Int. Ed.*, **2000**, 39, 1906.
6. Alami E., Levy H., Zana R., Skoulios A., *Langmuir*, **1993**, 9, 940.
7. Rosen M. J., Mathias J. H., Davenport L., *Langmuir*, **1999**, 15, 7340.
8. Zana R., Benrroua M., Rueff R., *Langmuir*, **1991**, 76, 1072.
9. Wettig S. D., Nowak P., Verrall R. E., *J. Colloid Interface Sci*, **2001**, 235, 310.
10. Wettig S. D., Nowak P., Verrall R. E., *Langmuir*, **2002**, 18, 5354.
11. Zana R., Talmon Y., *Nature*, **1993**, 362, 288.
12. Wennerstrom H., Lindman B., *Phys. Rep.* **1979**, 52, 1.
13. Menger F. M., *Angew Chem. Int. Ed. Engl.* **1991**, 30, 1086.
14. Bunton C. A., Robinson L., Schaak J., Stern M. F., *J. Org. Chem.*, **1971**, 36, 2346.
15. Vinson P. K., Bellare J. R., Davis H. T., Miller W. G., Scriven L. E., *J. Colloid Interface Sci.*, **1991**, 74, 142.
16. Appell J., Poyte G., Khatory A., Kem F., Candau S. J., *J. Phys. (France)*, **1992**, 2, 1045.
17. Hirata H., Sato M., Sakaiuchi Y., Katsube Y., *J. Colloid Polym. Sci.*, **1988**, 266, 862.
18. Jaeger D. A., Li B., Clark T. Jr., *Langmuir*, **1996**, 12, 4314.
19. Danino D., Talmon Y., Zana R., *Langmuir*, **1995**, 11, 1448.
20. Zana R., *Structure –Performance relationship in surfactants*, Esumin K., Ueno M., (Eds.), M. Dekker Inc, New York, **1997**.
21. Wang X., Wang J., Yan H., Li P., Thomas R. K., *Langmuir*, **2004**, 20, 53.
22. Wettig S. D., Li X., Verrall R. E., *Langmuir*, **2003**, 19, 3666.
23. Hirata H., Hattori N., Ishida M., Okabayashi H., Frusaka M., Zana R., *J. Phys. Chem.*, **1995**, 99, 17778.

24. Zana R., *Advances in Colloid and Interface Sci.*, **2002**, 97, 203.
25. Dreja M., Pyckhout-Hintzen W., Mays H., Tieke B., *Langmuir*, **1999**, 15, 391.
26. Zana R., *J. Colloid Interface Sci.*, **2002**, 252, 259.
27. Zhao J., Christian S. D., and Fung B. M., *J. Phys. Chem. B*, **1998**, 102, 761.
28. Perez L., Torres J. L., Manresa A., Solans C., Infante M. R., *Langmuir*, **1996**, 12, 5296.
29. De S., Aswal V. K., Goyal P. S., Bhattacharya S., *J. Phy. Chem.*, **1996**, 100, 11664.
30. Nusselder J. J. H., Engberts J. B. F. N., *J. Colloid Interface*, **1992**, 148, 353.
31. Schmitt V., Schosseler F., Lequeux F., *Europhys. Lett.*, **1995**, 30, 31.
32. Oda R., Panizza P., Schmutz M., Lequeux F., *Langmuir*, **1997**, 13, 6407.
33. Camesano T. A., Nagarajan R., *Colloids and Surfaces A*, **2000**, 167, 165.
34. Shah D. O., *J. Colloid Interface Sci.*, **1971**, 37, 744.
35. Jonsson, B. Lindman, K. Holmberg, B. Kmnnberg, *Surfactants and polymer in aqueous solution*, Wiley, New York, **1998**.
36. Patist, I. Axlclberd, D. O. Shah, *J. Colloid Interface Sci.*, **1998**, 208, 259.